Evidence for the molecular-scale origin of the suppression of physical ageing in confined polymer: fluorescence and dielectric spectroscopy studies of polymer–silica nanocomposites

Evidence for the molecular-scale origin of the suppression of physical ageing in confined polymer: fluorescence and dielectric spectroscopy studies of polymer–silica nanocomposites

Rodney D Priestley[1]**, Perla Rittigstein**[1]**, Linda J Broadbelt**[1]**, Koji Fukao**[2,4] **and John M Torkelson**[1,3,4]

[1] Department of Chemical and Biological Engineering, Northwestern University, Evanston, IL 60208, USA
[2] Department of Polymer Science and Engineering, Kyoto Institute of Technology, Kyoto 606-8585, Japan
[3] Department of Materials Science and Engineering, Northwestern University, Evanston, IL 60208, USA

E-mail: fukao@kit.ac.jp and j-torkelson@northwestern.edu

Abstract

Fluorescence spectroscopy was used to characterize the rate of physical ageing at room temperature in nanocomposites of silica (10–15 nm diameter) nanoparticles in poly(methyl methacrylate) (PMMA). The physical ageing rate was reduced by more than a factor of 20 in 0.4 vol% silica–PMMA nanocomposites relative to neat PMMA. The molecular-scale origin of this nearly complete arresting of physical ageing was investigated with dielectric spectroscopy. The strength of the β relaxation process was reduced by nearly 50% in the nanocomposite relative to neat PMMA. This reduced strength of the β process results from dipoles (ester groups) having hindered motions or being virtually immobile on the timescale being probed at a frequency of 100 Hz. This hindered mobility results from hydrogen bonding between PMMA ester side groups and hydroxyl units on the surface of the silica nanoparticles. In contrast, no reduction in physical ageing rate was observed upon addition of silica to polystyrene, which cannot form hydrogen bonds with the silica surfaces. Thus, the molecular origin of the suppressed physical ageing in silica–PMMA nanocomposites is the interfacial hydrogen bonding, which leads to a major reduction in the strength of the β process, i.e., the β process is largely responsible for the observed physical ageing.

[4] Authors to whom any correspondence should be addressed.

1. Introduction

When confined to the nanoscale, polymer films often exhibit a substantial deviation in the glass transition temperature (T_g) compared to the bulk state [1–27]. The observed changes in T_g with decreasing film thickness, which have been reported to be as large as 45–50 K in supported polymer films [14] and even greater in the case of freely standing films [2], are commonly attributed to the presence of interfacial effects perturbing T_g dynamics in ultrathin films [1, 2, 5, 6, 8, 10, 11, 15, 16, 20]. For supported films, interfacial effects arise from the free surface (polymer–air interface) and the substrate interface. The free surface generally acts to reduce the requirement for cooperative segmental mobility while attractive interactions at the substrate can increase the requirement for cooperative segmental mobility associated with T_g. In general, for supported polymer films experiencing increasing nanoconfinement, T_g decreases in films that lack attractive interactions with the substrate (e.g. polystyrene (PS) on silica) [1, 4, 6, 8, 11, 14, 18] and increases in films with significant attractive polymer–substrate interactions (e.g. poly(methyl methacrylate) (PMMA) on silica with silanol units on the substrate surface) [1, 6, 10, 12]. Exceptions to this general rule have been demonstrated in silica-supported films of particular compositions of styrene/methyl methacrylate random copolymers [18, 26] and of PS or PMMA containing 4 wt% of selected, low molecular weight diluents [13, 25]. Such systems exhibit no apparent impact of nanoconfinement on the average T_g across the film [13, 18, 25]. In the case of the random copolymer system, this exception may be understood to arise from an approximate cancelling of the opposing perturbations to T_g by the free surface and substrate effects; in the case of the films containing low MW diluent, this exception may be understood to arise from diluents reducing the size scale of cooperative rearranging regions [13] or reducing the length scale at which the free surface affects polymer dynamics [19].

Recently, there has been significant interest in the effect of nanoscale confinement on the sub-T_g relaxation or 'physical ageing' of polymer films [8, 28–34]. Physical ageing is the observed spontaneous change in properties as a function of annealing time below T_g [35–41]. In bulk polymers, this leads to time-dependent properties including increases in density, modulus, and yield stress, and decreases in specific enthalpy, impact strength, fracture energy, and ultimate elongation. The molecular motions associated with physical ageing are believed to be the small scale subsegmental flexible groups in the polymer backbone or the flexible side groups [35]. These motions are considered to be the manifestation of the β relaxation process in polymers. In the case of PS supported on silica, it has been observed that physical ageing can be suppressed by nanoconfinement in a limited set of conditions. In ultrathin films at temperatures below $T_{g,\text{bulk}}$, physical ageing is arrested or absent when the film T_g is sufficiently reduced by nanoconfinement that it is below the experimental temperature [28, 30]. This must be the case because by definition physical ageing cannot occur when an amorphous material is in its rubbery or liquid state. In contrast, at a constant depth ($T_{g,\text{film}} - T_{\text{ageing}}$) below T_g [30], 20 nm thick and 500 nm thick PS films supported on silica exhibit the same ageing rate, indicating that when the effect of nanoconfinement on T_g is accounted for there is no effect of nanoconfinement on ageing rate. Very different results have been obtained with ultrathin PMMA films supported on silica. When aged deep in the glassy state, the ageing rate of this system is vastly reduced with nanoconfinement [29, 30]. Employing a novel fluorescence/multi-layer experimental protocol, it was also shown in a bulk PMMA film at $T_g - 88$ K that physical ageing is nearly arrested within 25 nm of the substrate interface and that the ageing rate is reduced relative to the bulk state at length scales exceeding 100 nm from the substrate interface [29]. It was hypothesized that strong hydrogen bonding interactions between the ester groups on PMMA and the hydroxyl groups on silica impeded the relaxations associated with physical ageing.

Effects of nanoconfinement on T_g and physical ageing of polymers are not unique to the thin-film geometry [42–48]. As with ultrathin polymer films, confinement effects in polymer–nanosphere nanocomposites can lead to decreases or increases in T_g relative to the neat polymer [42, 43]. The change in T_g depends on whether the nanocomposite formation leads to free surfaces between the polymer and nanoparticles or to wetted nanoparticle interfaces with attractive polymer interactions [43]. Confinement effects in nanocomposites can also perturb the physical ageing response of the polymer. For example, enthalpy relaxation has been reported to be nearly a factor of four smaller during ageing of a 10 parts per hundred epoxy–clay nanocomposite compared to that of neat epoxy [44]. Also, it was recently shown that physical ageing deep in the glassy state can be nearly arrested in 0.4 vol% silica–poly(2-vinyl pyridine) (P2VP) nanocomposites [43].

Here we describe the first study to characterize quantitatively the effect of confinement both in strongly suppressing physical ageing and in modifying the polymer α and β relaxation dynamics, i.e., cooperative segmental mobility associated with T_g and small-scale, subsegmental secondary relaxations, respectively. We have used silica–PMMA nanocomposites in which the 10–15 nm diameter silica nanospheres, present at 0.4 vol% or less, are well dispersed in the polymer. Fluorescence spectroscopy was used to provide a measure of physical ageing rate that is sensitive to nanoscale volume relaxation within the polymer [29, 30, 43, 49, 50] while dielectric spectroscopy was used to characterize the polymer α and β relaxation dynamics. At room temperature deep in the glassy state, the presence of 0.4 vol% silica nanospheres dispersed in PMMA reduces the physical ageing rate by more than a factor of 20. The results of our dielectric studies indicate that a reduction in the strength of the β relaxation dynamics (in the case of PMMA, the mobility of the ester side groups) is the molecular-scale origin of this remarkable suppression of physical ageing by confinement effects involving attractive polymer–substrate or polymer–nanofiller interactions.

2. Experimental procedure

2.1. Fluorescence spectroscopy

The fluorescence chromophore 4-tricyanovinyl-[N-(2-hydroxyethyl)-N-ethyl]aniline (TC1) was synthesized following procedures given in [51] and [52]. Using procedures outlined in [53], PMMA was synthesized by free radical polymerization, incorporating a trace level of TC1-labelled methacrylate monomer ($M_n = 150\,000$ g mol^{-1}, $M_w/M_n = 1.60$, by gel permeation chromatography using universal calibration with polystyrene standards; 0.24 mol% TC1-labelled methacrylate monomer incorporated in the polymer, by UV–vis absorbance). Bulk T_gs were measured by differential scanning calorimetry (DSC) (Mettler-Toledo DSC 822, second heat, onset method, 10 K min^{-1} heating rate) and also via fluorescence methods [8, 11, 13, 14], which were found to yield identical values of 393 K. Silica nanospheres (colloidal silica in methyl ethyl ketone, Nissan Chemical Industries, reported diameter of 10–15 nm) were used as received.

Thin films of neat PMMA (with TC1 label) and of silica–PMMA (with TC1 label) nanocomposites were prepared by spin coating [54, 55] dilute solutions of labelled PMMA in methyl ethyl ketone (MEK), with or without nanofiller, on quartz slides. Solutions containing nanofiller were sonicated (Branson 1200 sonicator) for 40 min prior to spin coating. Resulting films were at least 1 μm thick as determined using a Tencor P10 profilometer. Films were dried in a chemical fume hood for at least 2 days at room temperature prior to performing fluorescence measurements. The T_g of the 0.4 vol% silica–PMMA nanocomposite system was determined to be 399 K, as previously reported [43]. This method of preparing silica–

polymer nanocomposites yields well dispersed silica nanoparticles in polymers such as P2VP and PMMA [43, 56].

Before each physical ageing experiment, the thermal history was erased by annealing at 423 K for 1 h. Films were quenched to the ageing temperature of 296 K using a temperature-controlled cell holder preset to the ageing temperature. Fluorescence was measured using a Photon Technology International fluorimeter in front-face geometry with 2.5 mm excitation and emission slits (10 nm and 5 nm band-pass, respectively) and an excitation wavelength of 480 nm. Fluorescence was monitored by measuring the maximum emission intensity, 560–565 nm for neat PMMA (with TC1 label) and 584–588 nm for the 0.4 vol% silica–PMMA (with TC1 label) nanocomposite, as a function of ageing time after quenching the films from 423 K to the ageing temperature of 296 K.

2.2. Dielectric spectroscopy

The PMMA was synthesized by free radical polymerization (M_n = 355 000 g mol^{-1}, M_w/M_n = 1.54, by gel permeation chromatography using PS standards and universal calibration). The T_g = 394 K, as determined by DSC (Mettler-Toledo DSC 822, second heat, onset method, 10 K min^{-1} heating rate). Silica nanospheres are identical to those described above in section 2.1.

Films of neat PMMA and PMMA nanocomposites were prepared by spin coating [54, 55] dilute solutions of PMMA in MEK, with or without silica nanospheres, onto Al-deposited glass substrates. Solutions containing nanofiller were sonicated for 40 min prior to spin coating. The films were then annealed in vacuum for 12 h at 413 K. After annealing, Al was vacuum deposited on top of the films to serve as an upper electrode. Vacuum deposition of Al might increase the temperature of the films locally, which could cause dewetting. However, this issue is avoided in the present study since all films are greater than 3 μm in thickness. Film thickness (d) was measured using profilometry (Tencor P10) by taking the average of three measurements near the top electrode of the sample.

Dielectric relaxation spectroscopy measurements were performed using an *LCR* meter (HP4284A) in the frequency range from 20 Hz to 1 MHz. The sample cell was cycled from 253 to 433 K at a constant rate of 0.5 K min^{-1}. Dielectric measurements during heating and cooling were performed repeatedly. All data were reproducible after the first heating and cooling cycles. Data are reported from the second cooling cycle.

The geometrical capacitance is given by $C_o = \varepsilon_0(S/d)$, where ε_0 is the permittivity of vacuum and S is the effective area of the electrode ($S = 1.55 \times 10^{-5}$ m^2). From the geometrical capacitance, the loss component of the permittivity of a film (ε'') can be determined from $C'' = \varepsilon'' C_o$, where C'' is the loss component of the complex electrical capacitance.

3. Results and discussion

3.1. Fluorescence spectroscopy

Figure 1(a) shows the emission spectrum of a bulk, neat TC1-labelled PMMA film at two physical ageing times after quenching from above T_g to an ageing temperature of 296 K. After absorption of light and promotion of an electron to an excited electronic state, the 'rotor' dye TC1 returns to the ground state by internal conversion (energy loss by vibrational and rotor motions) or fluorescence [29, 30, 49, 50, 57, 58]. Slight densification of the material occurs upon ageing, reducing the internal conversion and yielding an increase in fluorescence intensity.

Figure 1(b) compares the change in the fluorescence of the TC1 labels as a function of logarithmic physical ageing time for films of neat PMMA and 0.4 vol% silica–PMMA
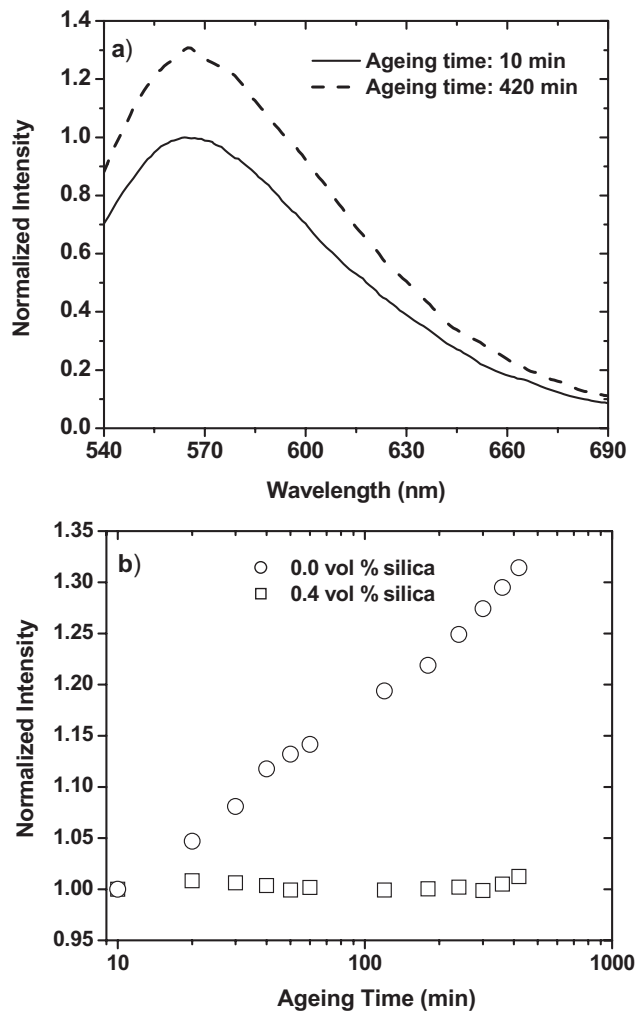
Figure 1. (a) Fluorescence emission spectrum of a bulk TC1-labelled PMMA film after quenching from 423 to 296 K taken after ageing times of 10 min (solid curve) and 420 min (dashed curve). (b) Normalized fluorescence intensity as a function of logarithmic ageing time for both neat PMMA (circles) and 0.4 vol% silica–PMMA nanocomposite (squares) aged at 296 K.

nanocomposites at 296 K. At this ageing temperature (which is $T_{g,bulk} - 97$ K for the PMMA film and $T_{g,bulk} - 103$ K for the nanocomposite film), the neat PMMA film shows a ∼31% increase in fluorescence intensity over 8 h. However, there is a much reduced effect of ageing time on fluorescence in the 0.4 vol% silica–PMMA nanocomposite, which exhibits a ∼1% increase in fluorescence intensity over 8 h.

From the plot in figure 1(b), a fluorescence physical ageing rate, R_f, can be defined in analogy with a physical ageing rate based on volume relaxation, R_v. During physical ageing, specific volume exhibits a roughly linear decrease with logarithmic ageing time, and the slope of the linear portion of this relation is defined as R_v [35–39]:

$$R_v = -v^{-1}[dv/d(\log t_a)] \tag{1}$$

where v is the specific volume and t_a is the ageing time. Because fluorescence intensity increases with a decrease in specific volume during physical ageing, R_f can be defined as follows [29, 30, 49, 50]:

$$R_f = f_o^{-1}[\mathrm{d}f/\mathrm{d}(\log t_a)] \tag{2}$$

where $f(f_o)$ is the fluorescence intensity at t_a ($t_a = 0$). Previous studies by Royal and Torkelson [49, 50], who used rotor fluorescence dyes to characterize physical ageing in bulk PS, PMMA, poly(vinyl acetate), polycarbonate and poly(isobutyl methacrylate), showed that the temperature dependence of the fluorescence physical ageing rate agreed with that of volume physical ageing rate and that the times required to reach equilibrium via enthalpy relaxation studies are similar to those of fluorescence physical ageing studies.

Using equation (2), we find that the physical ageing rate at 296 K is reduced by more than a factor of 20 in the 0.4 vol% silica–PMMA nanocomposites relative to neat PMMA. Specifically, with the units of t_a in minutes, $R_f = 0.19$ in PMMA, while $R_f = 0.008$ in the 0.4 vol% silica–PMMA nanocomposite. This extraordinary suppression in ageing rate is consistent with a previous report of arrested physical ageing in 0.4 vol% silica–P2VP nanocomposites [43] and with studies examining the physical ageing rates, both average values and their distributions, across thin PMMA films supported on one side by a silica (quartz) slide [29, 30]. Such effects of arrested or suppressed ageing are not found in ultrathin PS films [30] or 0.4 vol% silica–PS nanocomposites [56]. The current and previous results strongly indicate that the arrested or suppressed physical ageing is correlated to hydrogen bonds that can form between hydroxyl units that are naturally on the surface of silica slides or silica nanoparticles and groups on the polymer (e.g., the oxygen atoms in the ester side group in PMMA or the nitrogen atom in the ring structure in P2VP). When attractive polymer–substrate or polymer–nanofiller interactions are not possible, as in the case of PS, which contains no atoms that will form hydrogen bonds with hydroxyl groups, no suppression of ageing is evident within experimental error.

While the correlation between attractive polymer–nanofiller (substrate) interactions and suppressed physical ageing is clear, there has been no molecular-level explanation for how physical ageing rates can be so strongly suppressed throughout polymer nanocomposites (thin films), including regions where the polymer segments are some tens of nanometres removed from the polymer–nanofiller (substrate) interface. Below, we present results of dielectric relaxation spectroscopy measurements of silica–PMMA nanocomposites to address this issue.

3.2. Dielectric spectroscopy

Figure 2 shows the temperature dependence of the imaginary component of the complex dielectric constant (ε'') at a fixed frequency ($f = 100$ Hz) for both neat PMMA and 0.1 vol% silica–PMMA nanocomposite. The value of ε'' is normalized to the maximum value for each curve. Due to the presence of both the α and β processes, the imaginary part of the dielectric constant exhibits two maxima, with the peak temperatures denoted as T_α and T_β. In general, the molecular motions associated with the α process are attributed to cooperative segmental motions of the polymer, while the motions of the β process are associated with smaller, sub-segmental flexible groups in the polymer chain or flexible side groups [5, 35]. As can be seen in figure 2, the values of both T_α and T_β are impacted by the addition of silica nanofiller into PMMA. When $f = 100$ Hz, $T_\alpha = 409$ K and $T_\beta = 331$ K for neat PMMA, and $T_\alpha = 411$ K and $T_\beta = 329$ K for 0.1 vol% silica–PMMA nanocomposite. In addition, the widths of both the α and β processes increase slightly with the addition of nanofiller. (To obtain the most precise values, employing data of the type in figure 2, we extracted the peak temperatures of the α and β processes and their widths ΔT_α and ΔT_β by fitting the imaginary component of
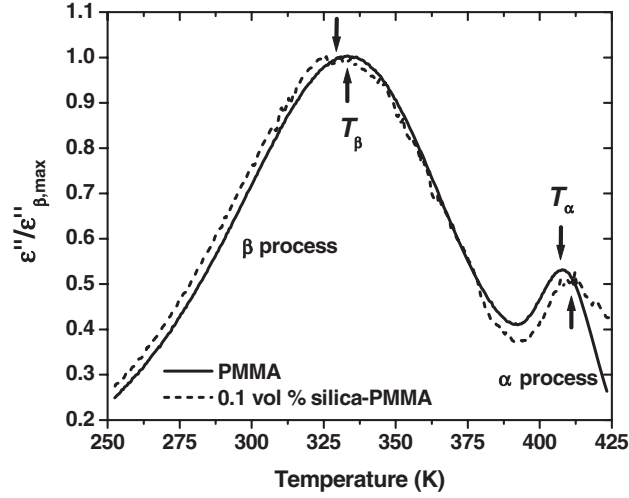
Figure 2. Temperature dependence of the imaginary component of the complex dielectric constant at 100 Hz for both neat PMMA (solid curve) and 0.1 vol% silica–PMMA nanocomposite (dashed curve). The vertical axis is normalized to the maximum value of each curve.

the dielectric constant as a function of temperature by the sum of two Lorentzian functions [5]: $\varepsilon_i'' / (1 + [(T - T_i)/\Delta T_i]^2)$, where $i = \alpha, \beta$.)

For ultrathin PMMA films supported between two Al electrodes, it has been reported that the value of T_α decreases with decreasing film thickness [5, 7]. In these studies the decrease in T_α with confinement was attributed to interfacial regions with enhanced dynamics compared to the bulk. In the current study, in which the films are at least 3 μm thick, the increase in T_α is related to the presence of the silica nanospheres. The increase in T_α with a simultaneous decrease in T_β of silica–PMMA nanocomposites is consistent with earlier reports of an increase in T_α and a decrease in T_β of PMMA confined in silica nanopores [47, 48]. For ultrathin atactic PMMA films supported between two Al electrodes, a decrease in T_β and broadening of T_β have been reported, both of which are consistent with the current findings [5].

Figure 3 compares the effects of increasing silica content, i.e. increasing confinement, on T_α data obtained in the present study with T_g data determined previously using fluorescence spectroscopy [43]. (Due to enhanced direct-current conductivity in 0.3 and 0.4 vol% silica–PMMA nanocomposites, the α relaxation peak was broadened, making it impossible to accurately determine T_α.) Both T_α ($f = 100$ Hz) and T_g increase slightly with the addition of silica nanofiller to PMMA. The increases in T_α and T_g with increasing silica content are consistent with previous reports of ultrathin PMMA films supported on silica substrates that show an enhanced T_g relative to the bulk value [1, 6, 12]. The increases in T_α and T_g may result from a reduction in mobility due to the hydrogen bonding interactions of the PMMA ester groups and the hydroxyl groups on silica [1].

The impact of silica nanofiller content on T_β and ΔT_β is given in figure 4. The width of the β process for each nanocomposite, ΔT_β, is normalized to that of neat PMMA, $\Delta T_{\beta,0}$. With increasing silica content, i.e., increasing confinement, the width of the β process increases while T_β slightly decreases. These findings are consistent with earlier work reported for thin PMMA films [5] and PMMA confined in silica nanopores [47, 48]. The solid line in figure 4 is a fit of the data to the following equation:

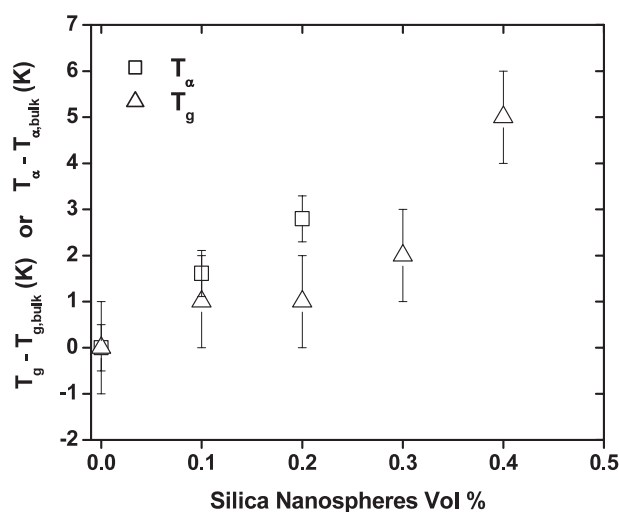$$\Delta T_\beta(\phi) = \Delta T_{\beta,0}(1 + \phi/a) \tag{3}$$

Figure 3. Effect of silica nanosphere content on T_α and T_g of PMMA. T_g data are from [43]. For neat PMMA, $T_\alpha = 409$ K and $T_g = 393$ K.
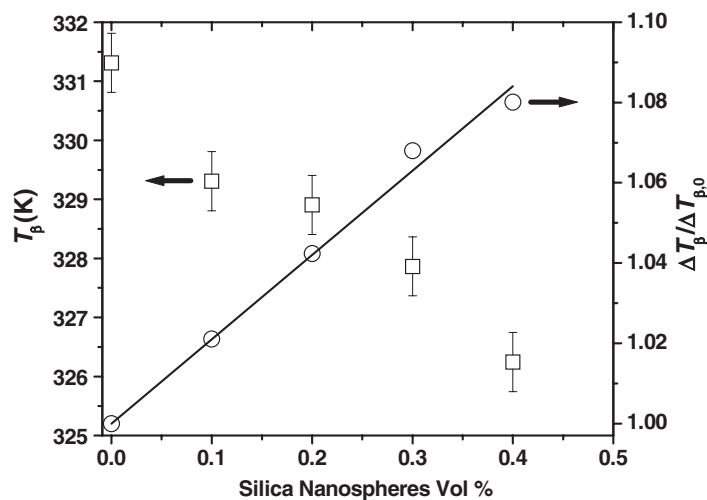

Figure 4. Effect of silica nanosphere content on T_β (squares) and the width of the β process normalized to that present in neat PMMA $\Delta T_\beta / \Delta T_{\beta,0}$ (circles). The solid line is a fit of the data to $\Delta T_\beta(\phi) = \Delta T_{\beta,0}(1 + \phi/a)$, where $\Delta T_{\beta,0} = 47$ K, $a = 4.7$ vol%, and ϕ is the volume per cent of silica nanofiller in the nanocomposite.

where $\Delta T_{\beta,0} = 47$ K, $a = 4.7$ vol%, and ϕ is the volume per cent of silica nanofiller in the nanocomposite. This equation is analogous (with a/d replacing ϕ/a) to one used earlier [5] in analysing the β process in thin and ultrathin PMMA films. Our value of $\Delta T_{\beta,0}$ obtained from the fit agrees well with that measured for the neat PMMA film employed in this study and that obtained in earlier work on thin and ultrathin PMMA films [5].

The broadening of ΔT_β with increasing silica content is likely related to an addition to the polymer dynamic heterogeneity inherently present in neat PMMA resulting from the attractive polymer–silica interactions reducing the mobility of some PMMA ester groups.
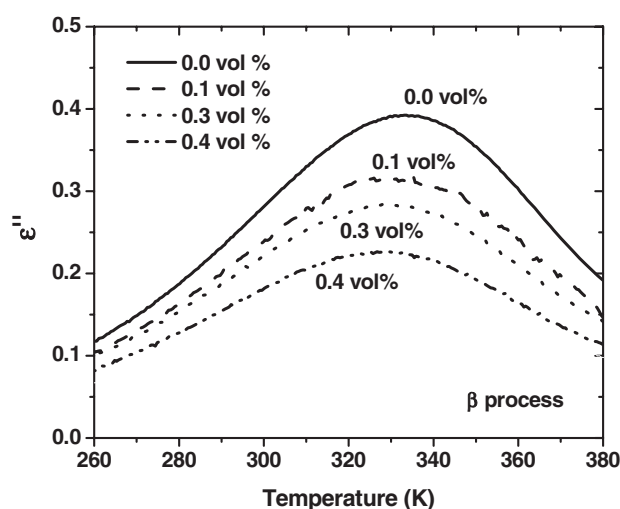
Figure 5. Effect of temperature on the dielectric loss constant of the β process for neat PMMA (solid curve), 0.1 vol% silica–PMMA nanocomposite (dashed curve), 0.3 vol% silica–PMMA nanocomposite (dotted curve), and 0.4 vol% silica–PMMA nanocomposite (dashed/dotted curve).

This is consistent with figure 2 which shows that addition of silica to PMMA leads to some broadening on the low temperature side of the β process. The slight reduction in T_β (shift to lower temperature of the peak maximum in figure 2) with increasing silica content may be related to the *faster* component of the β process having a relatively more intense contribution to the overall relaxation process, since slower components of the relaxation may be hindered or completely immobile as discussed below [48].

Finally, in order to examine the impact of nanofiller content on the strength of the β process, ε'' is evaluated as a function of temperature at a fixed frequency ($f = 100$ Hz) (see figure 5). While the addition of silica nanofiller to PMMA leads to a *slight* decrease in T_β, it results in a *major* reduction in the value of ε'' over all temperatures accessed in this study. In particular, when 0.4 vol% silica is dispersed in PMMA, the maximum value of ε'' is reduced by nearly 50% relative to the value in neat PMMA. The strength of the ε'' signal, i.e., its magnitude, is related to a complex combination of the density of fluctuating dipoles, the extent to which each dipole is able to fluctuate and the dipole moment of PMMA. Since the dipole moment of PMMA remains unchanged when 0.4 vol% silica is added to PMMA, the decrease in ε'' results from a combined effect, with some dipoles having hindered motion and some being immobile on the timescale being probed at a frequency of 100 Hz. (We note that while there is a slight decrease in T_β with increasing silica content, which, other things being equal, suggests a slight increase in the dynamics of the β process, the strength of the β process is vastly reduced. Thus, there is a major reduction in the extent to which the β relaxation occurs.)

The notion that the molecular motions associated with the β process are hindered or immobilized supports the idea that strong, attractive polymer–silica substrate interactions (in the case of thin films) and strong, attractive polymer–silica nanofiller interactions (in the case of nanocomposites) impede the relaxations associated with physical ageing, giving rise to the remarkable reduction in ageing rate observed in these nanoconfined systems. The hydrogen bonding interactions that occur between PMMA and silica involve the ester side groups on PMMA and the hydroxyl groups on silica. If the flexible side group motions of PMMA that contribute to physical ageing are hindered or immobilized by the presence of silica, it is logical

to interpret that the reduction in physical ageing rate observed in both PMMA films supported on silica [29, 30] and silica–PMMA nanocomposites is a consequence of a reduction in the mobility of the flexible side groups (motions associated with the β process). The concept that relaxations accompanying physical ageing are linked to the β relaxation process was established in bulk polymers nearly 30 years ago [35]. For PMMA, we note that a reduction in the strength of the β process was observed with decreasing film thickness for films supported between two Al electrodes [5, 27]. The reduction in the strength of the β process was attributed to a modification of the chain equilibrium conformational statistics [27]. This suggests that the reduced strength of the β process in the silica–PMMA nanocomposites may be due to a combination of effects related to the reduced mobility of the flexible side groups caused by hydrogen bonding interactions and by modified chain conformational statistics. Further study is warranted to address this issue.

While this study has made a strong connection between the reduced strength of the β process with the suppression of physical ageing in PMMA-silica nanocomposites, the mechanism by which the β process and thereby physical ageing is hindered over length scales of tens of nanometres away from the polymer–silica interface is as yet unknown. (If an idealized dispersion is assumed and the nanospheres are arranged in a cubic array, the theoretical interparticle distance of 0.4 vol% silica (10–15 nm in diameter) is ∼50 nm. Since the dispersion is not ideal, the average interparticle distance must be greater than ∼50 nm.) Does the long-range propagation of interfacial effects that hinder the β process and physical ageing have its origin in the fact that numerous silica nanoparticles distributed with 10–50 nm will impact the dynamics of a single polymer segment? Is there an effect of temperature relative to T_g on the length scale over which the effects of attractive interfacial interactions propagate away from the interface? These are but a few of the scientific questions associated with this behaviour. Besides the important scientific issues, the suppressed ageing observed in polymer nanocomposites with attractive polymer–substrate interactions also has very important technological implications. In particular, this behaviour suggests that it may be possible to produce glassy materials consisting of polymer with traces of nanofiller which exhibit little or no physical ageing, although the polymer itself is a non-equilibrium glass that ages significantly in the neat state.

4. Conclusions

Fluorescence spectroscopy has been used to determine the impact of silica nanofiller on the rate of physical ageing of PMMA, while dielectric relaxation spectroscopy has been used to determine the impact of silica nanofiller on the α and β relaxation processes. At room temperature, the addition of 0.4 vol% silica nanofiller to PMMA results in nearly total arrest of physical ageing during the experimental timescale measured. This addition of silica nanofiller also greatly reduces the strength of the β process in PMMA. We believe that these two effects are strongly correlated and that the reduction in the PMMA ester side group mobility that is the cause of the reduced strength of the β process is also a major part of the molecular-scale origin of the suppression of physical ageing in the silica–PMMA nanocomposites.

Acknowledgments

References

[1] Keddie J L, Jones R A L and Cory R A 1994 *Europhys. Lett.* **27** 59
[2] Forrest J A, Dalnoki-Veress K, Stevens J R and Dutcher J R 1996 *Phys. Rev. Lett.* **77** 2002
[3] Hall D B, Hooker J C and Torkelson J M 1997 *Macromolecules* **30** 667
[4] Fukao K and Miyamoto Y 2000 *Phys. Rev.* E **61** 1743
[5] Fukao K, Uno S, Miyamoto Y, Hoshino A and Miyaji H 2001 *Phys. Rev.* E **64** 051807
[6] Fryer D S, Peters R D, Kim E J, Tomaszewski J E, de Pablo J J and Nealey P F 2001 *Macromolecules* **34** 5627
[7] Hartmann L, Gorbatschow W, Hauwende J and Kremer F 2002 *Eur. Phys. J.* E **8** 145
[8] Ellison C J, Kim S D, Hall D B and Torkelson J M 2002 *Eur. Phys. J.* E **8** 155
[9] Grohens Y, Hamon L, Reiter G, Soldera A and Holl Y 2002 *Eur. Phys. J.* E **8** 217
[10] Sharp J S and Forrest J A 2003 *Phys. Rev.* E **67** 031805
[11] Ellison C J and Torkelson J M 2003 *Nat. Mater.* **2** 695
[12] Roth C B and Dutcher J R 2003 *Eur. Phys. J.* E **12** S103
[13] Ellison C J, Ruszkowski R L, Fredin N J and Torkelson J M 2004 *Phys. Rev. Lett.* **92** 095702
[14] Ellison C J, Mundra M K and Torkelson J M 2005 *Macromolecules* **38** 1767
[15] Peter S, Meyer H and Baschnagel J 2006 *J. Polym. Sci.* B **44** 2951
[16] Seemann R, Jacobs K, Landfester K and Herminghaus S 2006 *J. Polym. Sci.* B **44** 2968
[17] Ngai K L 2006 *J. Polym. Sci.* B **44** 2980
[18] Mundra M K, Ellison C J, Behling R E and Torkelson J M 2006 *Polymer* **47** 7747
[19] Riggleman R A, Yoshimoto K, Douglas J F and de Pablo J J 2006 *Phys. Rev. Lett.* **97** 045502
[20] Merabia S, Sotta P and Long D 2004 *Eur. Phys. J.* E **15** 189
[21] McCoy J D and Curro J G 2002 *J. Chem. Phys.* **116** 9154
[22] Baschnagel J and Varnik F 2005 *J. Phys.: Condens. Matter* **17** R851
[23] Alcoutlabi M and McKenna G B 2005 *J. Phys.: Condens. Matter* **17** R461
[24] Roth C B and Dutcher 2004 *Soft Materials: Structure and Dynamics* ed J R Dutcher and A G Marangoni (New York: Dekker)
[25] Mundra M K, Ellison C J, Rittigstein P and Torkelson J M 2007 *Eur. Phys. J. Special Topics* **141** 143
[26] Park C H, Kim J H, Ree M, Sohn B-H, Jung J C and Zin W-C 2004 *Polymer* **45** 4507
[27] Wubbenhorst M, Murray C A, Forrest J A and Dutcher J R 2002 *Proc. 11th Int. Symp. on Electrets* p 401
[28] Kawana S and Jones R A L 2003 *Eur. Phys. J.* E **10** 223
[29] Priestley R D, Ellison C J, Broadbelt L J and Torkelson J M 2005 *Science* **309** 456
[30] Priestley R D, Broadbelt L J and Torkelson J M 2005 *Macromolecules* **38** 654
[31] Fukao K and Sakamoto A 2005 *Phys. Rev.* E **71** 041803
[32] Cangialosi D, Wubbenhorst M, Groenewold J, Mendes E, Schut H, van Veen A and Picken S J 2005 *J. Non-Cryst. Solids* **351** 2605
[33] Huang Y and Paul D R 2004 *Polymer* **45** 8377
[34] Huang Y and Paul D R 2006 *Macromolecules* **39** 1554
[35] Struik L C E 1978 *Physical Aging in Amorphous Polymers and Other Materials* (Amsterdam: Elsevier)
[36] Greiner R and Schwarzl F R 1984 *Rheol. Acta* **23** 378
[37] Kovacs A J 1981 *Structure and Mobility in Molecular and Atomic Glasses* vol 371, ed J M O'Reilly and M Goldstein (New York: The New York Academy of Sciences) p 38
[38] Hutchinson J M 1995 *Prog. Polym. Sci.* **20** 703
[39] Hodge I M 1995 *Science* **267** 1945
[40] McKenna G B 1989 *Comprehensive Polymer Science* vol 2, ed C Booth and C Price (Oxford: Pergamon) p 311
[41] Angell C A, Ngai K L, McKenna G B, McMillian P F and Martin S W 2000 *J. Appl. Phys.* **88** 3133
[42] Ash B J, Schadler L S and Siegel R W 2002 *Mater. Lett.* **55** 83
[43] Rittigstein P and Torkelson J M 2006 *J. Polym. Sci.* B **44** 2935
[44] Lu H and Nutt S 2003 *Macromolecules* **36** 4010
[45] Anastasiadis S H, Karatasos K, Vlachos G, Manias E and Giannelis E P 2000 *Phys. Rev. Lett.* **84** 915
[46] Elmahdy M M, Chrissopoulou K, Afratis A, Floudas G and Anastasiadis S H 2006 *Macromolecules* **39** 5170
[47] Kalogeras I M and Neagu E R 2004 *Eur. Phys. J.* E **14** 193
[48] Kalogeras I M 2005 *Acta Mater.* **53** 1621
[49] Royal J S and Torkelson J M 1992 *Macromolecules* **25** 1705
[50] Royal J S and Torkelson J M 1993 *Macromolecules* **26** 5331
[51] Hooker J C 1996 *PhD Thesis* Northwestern University
[52] McKusick B C, Heckert R E, Cairns T L, Coffman D D and Mower H F 1958 *J. Am. Chem. Soc.* **80** 2806
[53] Deppe D, Dhinojwala A and Torkelson J M 1996 *Macromolecules* **29** 3898

[54] Spangler L, Royal J S and Torkelson J M 1990 *Polym. Eng. Sci.* **30** 644
[55] Hall D B, Underhill P and Torkelson J M 1998 *Polym. Eng. Sci.* **38** 2039
[56] Rittigstein P and Torkelson J M 2007 manuscript in preparation
[57] Loutfy R O and Arnold B A 1982 *J. Phys. Chem.* **86** 4205
[58] Loutfy R O and Teegarden D M 1983 *Macromolecules* **16** 452